Oxidation Resistance of Iron and Copper Foils Coated with Reduced Graphene Oxide Multilayers

Dongwoo Kang,[†] Jee Youn Kwon,[‡] Hyun Cho,[‡] Jae-Hyoung Sim,[‡] Hyun Sick Hwang,[‡] Chul Su Kim,[‡] Yong Jung Kim,[§] Rodney S. Ruoff,[⊥] and Hyeon Suk Shin[†,*]

[†]Interdisciplinary School of Green Energy, Low Dimensional Carbon Materials Center and KIER-UNIST Advanced Center for Energy, Ulsan National Institute of Science and Technology (UNIST), UNIST-gil 50, Ulsan 689-798, Republic of Korea, [‡]Daegu Science High School, Hwanggeum 2-dong, Daegu 706-852, Republic of Korea, [§]Division of Carbon Materials, Research Institute of Science and Technology, Private Box 135, Pohang 790-600, Republic of Korea, and [⊥]Department of Mechanical Engineering and the Materials Science and Engineering Program, The University of Texas at Austin, One University Station C2200, Austin, Texas 78712, United States

The protection of metal surfaces is important, and many approaches have been developed. Coating with other metal(s),[1] chemical modification,[2] anodizing,[3] using an oxide layer,[4] and organic layer/polymer coating are some examples.[5−8] Recently, graphene, which was successfully grown on large-area Cu substrates by a chemical vapor deposition (CVD) method,[9] was tested as a barrier and shown to protect Cu and Cu/Ni alloy surfaces from oxidation.[10,11] Fe, widely used in industry, can also be used for CVD graphene growth.[12,13] However, to date, uniform graphene layers have not been achieved on Fe substrates.[14] Reduced graphene oxide (rG-O), when deposited as a thin film, is an alternative candidate for protecting Fe and Cu surfaces because large thin films can be readily formed by a solution process.[15] Furthermore, rG-O can be easily synthesized in a large quantity by oxidation of natural graphite, followed by reduction with a wide variety of reducing (deoxygenating) agents or by thermal treatment.[16]

rG-O has been used in organic thin-film transistors (OTFTs) and field-effect transistors (FETs),[17,18] conducting transparent films,[15,19−24] sensors,[25,26] and energy storage materials,[27] but oxidation resistance of rG-O-coated metal surfaces to our knowledge has not been reported. We expected that rG-O multilayers might act as a diffusion barrier to gas molecules (including oxidants such as H_2O and O_2) and thus as a protective layer to prevent or slow oxidation in metals.

Herein semitransparent rG-O multilayers were fabricated on a SiO_2 (300 nm) deposited on Si substrate by layer-by-layer (LbL) assembly of negative and positive charged

ABSTRACT
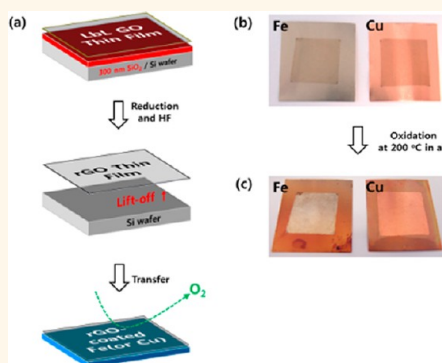
Protecting the surface of metals such as Fe and Cu from oxidizing is of great importance due to their widespread use. Here, oxidation resistance of Fe and Cu foils was achieved by coating them with reduced graphene oxide (rG-O) sheets. The rG-O-coated Fe and Cu foils were prepared by transferring rG-O multilayers from a SiO_2 substrate onto them. The oxidation resistance of these rG-O-coated metal foils was investigated by Raman spectroscopy, optical microscopy, and scanning electron microscopy after heat treatment at 200 °C in air for 2 h. The bare metal surfaces were severely oxidized, but the rG-O-coated metal surfaces were protected from oxidation. This simple solution process using rG-O is one advantage of the present study.

KEYWORDS: graphene oxide · reduced graphene oxide · iron · oxidation resistance · gas barrier

graphene oxide sheets, followed by thermal treatment.[28,29] The rG-O thin films were then transferred onto Fe and Cu foils to assess the oxidation resistance of these rG-O-coated metal surfaces. The possible oxidation of bare metal and rG-O-coated metal surfaces was investigated by Raman spectroscopy, optical microscopy, and scanning electron microscopy (SEM) before and after heating at 200 °C in air for 2 h.

It was found that the temperature used for thermal reduction (degree of reduction)
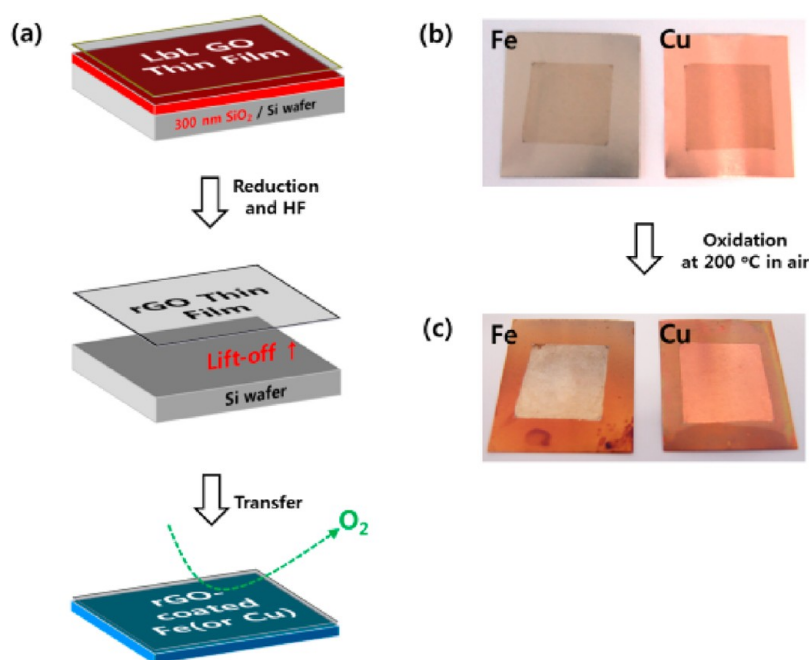
© XXXX American Chemical Society

Figure 1. (a) Schematic diagram for preparation of rG-O-coated metal. **(b, c)** Photographs of five-bilayer rG-O-coated Fe (left) and Cu (right) foils before and after oxidation by thermal treatment at 200 °C in air for 2 h.

and also the thickness of rG-O multilayers are factors affecting the degree of protection against oxidation of the metal surface. We concluded that the optimized condition for effective protection of the Fe or Cu surfaces from oxidation is five bilayers of rG-O and heat treatment above 800 °C for a suitable time as discussed further below. The advantage of using rG-O multilayers is that they are deposited by a solution process that is easy, reproducible, and transferrable to any substrate.

RESULTS AND DISCUSSION

Graphene oxide (G-O) suspensions were prepared by exfoliation of graphite oxide synthesized by the modified Hummers method.[30] The G-O sheets had an average lateral size of 8.34 μm and typical thickness of 0.8−1.0 nm, indicating that the majority of the sheets in the sample were single-layer (Figure S1 in the Supporting Information). The G-O suspension had good colloidal stability with a zeta-potential of less than −50 mV over a wide range of pH (Figure S2a in the Supporting Information). Negatively charged G-O sheets were converted into positively charged G-O sheets by reaction between the carboxylic acid groups of G-O and ethylene-diamine mediated with N-ethly-N′-(3-dimethylamino-propyl)carbodiimide methiodide;[29] the pH of the solution was adjusted to 3 to 4 with 0.1 M HCl. A well-dispersed and stable solution of positively charged G-O sheets was then obtained without agglomeration at a concentration of ∼0.4 mg/mL; the zeta potential was 50.2 mV at pH 3.7 (Figure S2a in the Supporting Information).

rG-O thin films on Si wafer substrates having a 300 nm thick thermal oxide layer were fabricated by repetitively spin-coating first the positively and then the negatively charged G-O solutions (LbL assembly) and thermal treatment. The LbL assembly allows for precise control of the thickness of the G-O thin films through the number of bilayers (see Figure S2b in the Supporting Information). The thickness of the rG-O thin films after thermal treatment was smaller than that of the G-O thin films. The decrease in thickness of the rG-O thin films was due to several factors, including removal of O-containing functional groups by heating and elimination of interlamellar water that was present in both graphite oxide and G-O thin films and that depended on relative humidity. The X-ray photoelectron spectroscopy (XPS) data (Figure S2c in the Supporting Information) show the extensive reduction in O-containing functional groups as a function of the temperature used for the deoxygenation. From the deconvolution of C 1s peaks in the XPS spectra, it was observed that C—O and C═O peaks at 286.8 and 288.5 eV dramatically decreased after the thermal reduction at 1100 °C, whereas the C═C peak at 284.8 eV increased (See deconvoluted C1s peaks of G-O and rG-O in Figure S2 in the Supporting Information.) Furthermore, the peak at 284.8 eV shifted to 284.4 eV as the temperature increased to 1100 °C. These results are in good agreement with previous literature.[29,31] The 8.8 nm thickness for five-bilayer G-O decreased to 3.3 nm after heating at 1100 °C for 1 h under vacuum (Ar 90 sccm and H$_2$ 10 sccm). It is also interesting that the interlayer spacing of the rG-O thin film after thermal treatment was very similar to that of crystalline graphite (see XRD data in Figure S3), and surface morphology became smooth after thermal treatment
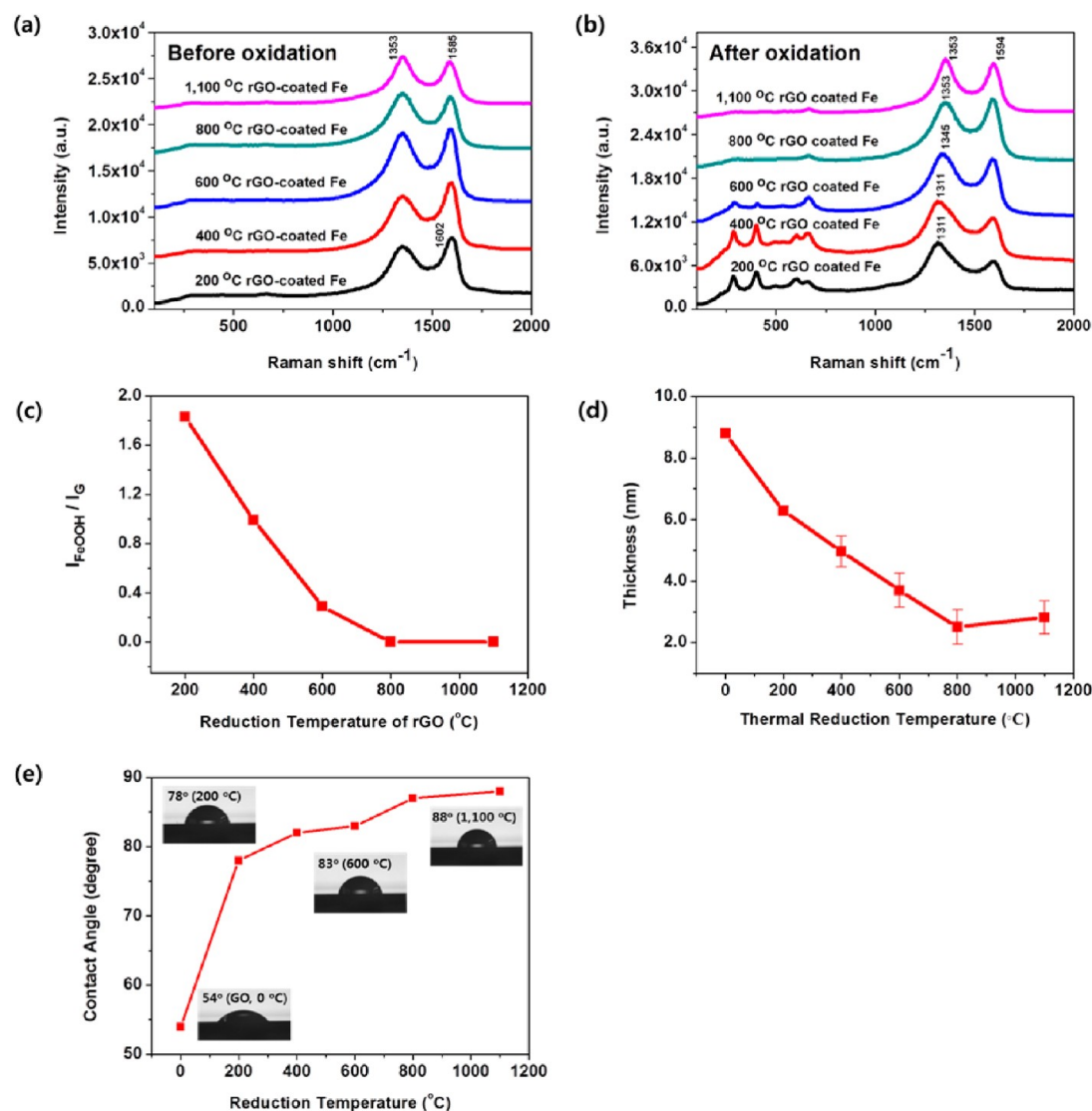
Figure 2. (a, b) Raman spectra before and after oxidation of five-bilayer rG-O-coated Fe at 200 °C in air for 2 h. The rG-O thin films were reduced at different temperatures from 200 to 1100 °C. (c) Ratio of I_{FeOOH}/I_G from spectra in (b). (d) Thickness change of five-bilayer rG-O films with an increase of reduction temperature. The film thickness was measured by ellipsometry. (e) Contact angles at different temperatures.

(see AFM data in Figure S4). Of course, crystallinity of the rG-O thin film is worse than graphite. This indicates that rG-O layers were well packed with removal of O-containing functional groups by thermal treatment at 1100 °C.

The rG-O thin films could also be obtained by reduction of the G-O thin films by hydrazine vapor at 100 °C, and hydrazine molecules and some N-functionalized groups remained in the rG-O multilayers (Figure S5 in the Supporting Information). The rG-O thin films obtained by exposure to hydrazine vapor were found to not protect Fe or Cu foil surfaces, and this is likely due to residual hydrazine molecules and defect sites (Figure S5). We thus focus discussion on the rG-O thin films prepared by thermal reduction as protective layers.

The scheme for the preparation of rG-O-coated metals and photographs of the five-bilayer rG-O-coated

Fe and Cu foils before and after oxidation are shown in Figure 1. The oxidation of Fe and Cu foils was done by heating them at 200 °C in air for 2 h. Apparently, it seems that the rG-O layers protect oxidation of Fe and Cu foils. (Evidence of the oxidation resistance will be provided using Raman spectroscopy, optical microscopy, and SEM later.) The rG-O layers were obtained by thermal reduction at 1100 °C as demonstrated above.

Raman spectra of rG-O-coated Fe foils before and after oxidation were measured to assess oxidation resistance. The rG-O-coated Fe foils were prepared at various reduction temperatures from 200 to 1100 °C. It is noted that a red shift of the G band was observed from 1602 to 1585 cm^{-1} as the reduction temperature increased (Figure 2a). Generally, a restored sp^2-hybridized graphitic carbon network by reduction at
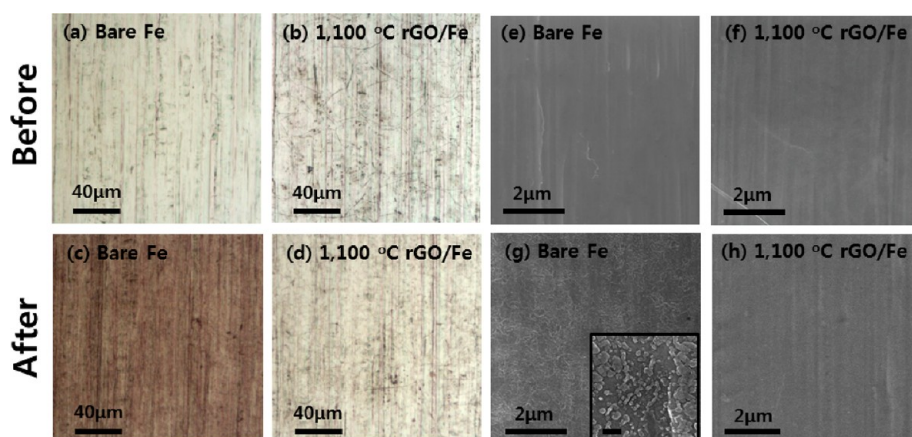
Figure 3. (a−d) Optical microscope (OM) images and (e−h) corresponding SEM images of bare and five-bilayer rG-O-coated Fe foils before and after oxidation at 200 °C in air for 2 h. The rG-O layer was obtained after thermal reduction at 1100 °C and transferred onto Fe foil. The inset in (g) is a magnified SEM image of bare Fe after oxidation, and the scale bar is 500 nm.

high temperature can lead to a shift of the G band,[32] which is consistent with our XPS data (Figure S2d in the Supporting Information). It is particularly note-worthy that various Raman bands due to iron oxide phases such as FeOOH (218, 285, 289, and 397 cm^{-1}), Fe_2O_3 (406, 657, and 670 cm^{-1}), and Fe_3O_4 (603 and 670 cm^{-1})[33,34] appeared in the spectral region of 100 and 800 cm^{-1} after oxidation of rG-O-coated Fe samples reduced at temperatures below 800 °C. On the other hand, there was no Raman band due to iron oxide phases after oxidation of rG-O-coated Fe samples reduced at 800 and 1100 °C (Figure. 2b). Note that a very weak band at 670 cm^{-1} was due to native iron oxide on Fe foil and appeared even in Raman spectra before oxidation in Figure 2a and in the Raman spec-trum of bare Fe foil in Figure S11. From Raman spectra in Figure 2b, the degree of oxidation of rG-O-coated Fe samples was investigated by calculating the Raman intensity ratio of a band at 397 cm^{-1} due to α-FeOOH (goethite: a kind of iron oxide) and the G band as an internal standard. Figure 2c shows the ratio I_{FeOOH}/I_G at different temperatures. The I_{FeOOH}/I_G values gradually decreased as the reduction temperature increased (1.83 at 200 °C, 0.99 at 400 °C, and 0.29 at 600 °C) and finally approached zero at 800 and 1100 °C. This result indicates that rG-O-coated Fe foils reduced at low temperature were heavily oxidized, whereas those at 800 and 1100 °C were protected from oxidation. Figure 2d shows thickness changes of the rG-O thin films as a function of the thermal reduction tempera-ture. It is interesting that the thickness of the rG-O thin films decreased with an increase of the reduction temperature, which is the same tendency as the change of the intensity ratio in Figure 2c. The thicker films reduced at temperatures of 200 to 600 °C were due to existing functional groups in the rG-O layers, which were not completely removed by the thermal treatment, so water and oxygen could permeate through the thick films. It appears that the partially

reduced G-O films did not play a role as a diffusion barrier of gas and did not protect the Fe surface from oxidation. Furthermore, the existing functional groups containing oxygen may accelerate oxidation of the Fe surface. On the other hand, the rG-O thin films reduced at 800 and 1100 °C are supposed to be well packed without functional groups (see XRD data in Figure S3) and so play a role as a barrier of gas (see Figure S6 in the Supporting Information for measurement of He gas permeability). It is known that water molecules perme-ate G-O membranes of 1 μm thickness but not a 1 μm thick rG-O membrane, whereas He gas does not permeate either 1 μm thick G-O or rG-O membranes.[35] However, it is difficult to compare these prior results with the rG-O multilayers films studied here, as they are very thin, less than 10 nm. We made attempts to measure the permeability to He gas but our thin rG-O films broke during attempts to mount them. The contact angle measurement in Figure 2e supports the existence of functional groups between 200 and 600 °C. The contact angle was 54° for G-O, 78° at 200 °C, 82° at 400 °C, 83° at 600 °C, 87° at 800 °C, and 88° at 1100 °C. As the temperature increased, the con-tact angle increased, indicating removal of oxygen-containing functional groups.[36,37]

The oxidation resistance of the rG-O layer was also confirmed by optical microscopy (OM) and SEM. Figure 3a−d show OM images of bare Fe and five-bilayer rG-O-coated Fe before and after oxidation. The color of the bare Fe changed to brown after oxidation, whereas the color of the rG-O-coated Fe remained unchanged after oxidation. Note that the color of the rG-O-coated Fe was slightly darker than that of the bare Fe due to the rG-O layer. SEM images also showed a noticeable difference between the bare Fe and the rG-O-coated Fe after oxidation. The bare Fe shows morphology of particulates after oxidation in Figure 3g, whereas the rG-O-coated Fe remains without a morphology change in Figure 3h. rG-O multilayers of one and three bilayers
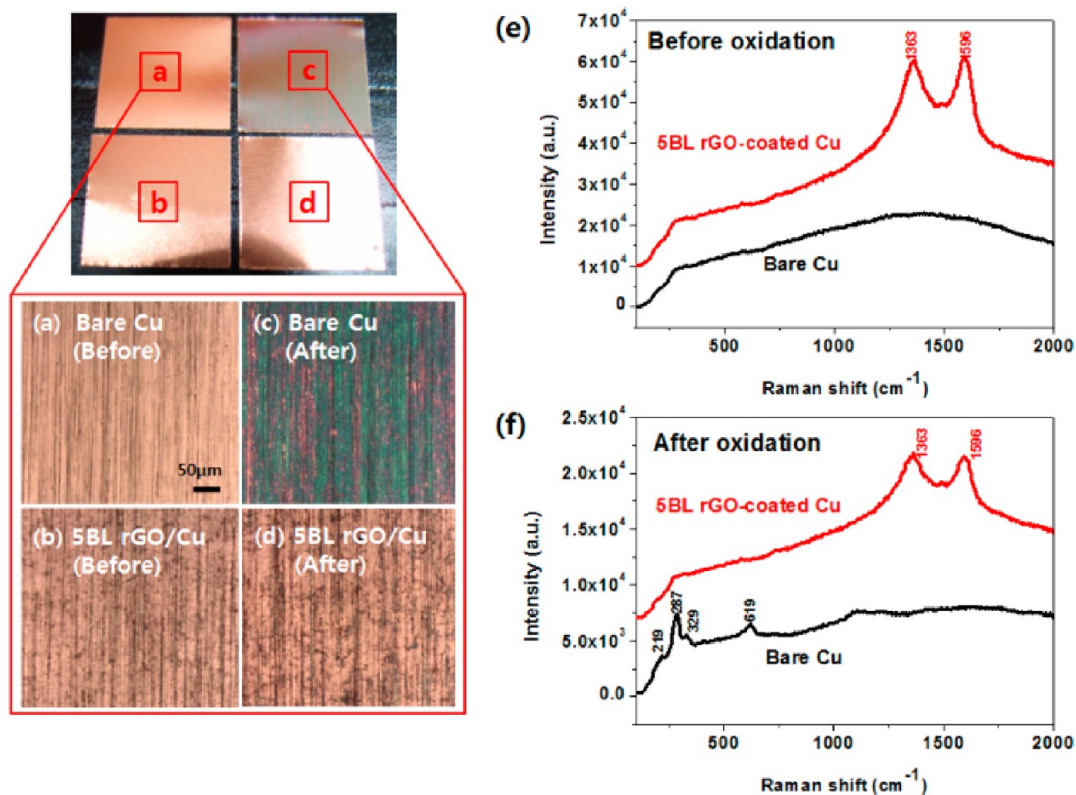
Figure 4. (a, b) Photographs and OM images of bare and five-bilayer rG-O-coated Cu foils before and (c, d) after oxidation at 200 °C in air for 2 h and (e, f) Raman spectra of each sample.

were ineffective as a gas barrier for oxidation resistance of metal possibly due to poor coverage. Among thicker rG-O films of 10, 15, and 20 bilayers, rG-O films of 15 and 20 bilayers were also ineffective as a gas barrier for oxidation resistance of Fe (see Figures S7–S10 in the Supporting Information). Thus, we reach a conclusion that five bilayers in rG-O multilayers is either the optimum or close to the optimum thickness for oxidation resistance and optical transparency: the five-bilayer film is more transparent than a 10-bilayer-thick film.

The oxidation resistance of the rG-O layer can be applied to Cu foil. The preparation method of the rG-O layer and the oxidation procedure for Cu foil were identical to those for Fe foil. Figure 4a–d show photographs and OM images of bare Cu and rG-O-coated Cu. The color of the bare Cu turned greenish after oxidation, whereas the color of the rG-O-coated Cu remained unchanged. Note that the color of the rG-O-coated Cu is slightly darker than that of the bare Cu.

The comparison of Raman spectra before and after oxidation in Figure 4e, f also revealed that the rG-O layer successfully protected the Cu surface. The Raman spectrum of the bare Cu after oxidation shows some bands due to copper oxides such as Cu_2O (219 cm^{-1}) and CuO (287, 329, and 619 cm^{-1}).[38,39] On the other hand, the Raman spectrum of the rG-O-coated Cu after oxidation did not show any band in the spectral region. Note that two large Raman bands between 1250 and 1700 cm^{-1} are called D and G bands and originated from the rG-O layer.

CONCLUSIONS

The rG-O multilayers using layer-by-layer assembly were successfully fabricated and transferred to Fe and Cu foils. The oxidation resistance of Fe and Cu foils by the rG-O layers was confirmed by Raman spectroscopy, optical microscopy, and SEM. The results mean that the rG-O layers play a role as a diffusion barrier of gas. The solution process using rG-O is easy and reproducible.

METHODS

Preparation of Graphene Oxide (G-O). Graphite oxide was prepared from purified natural graphite (SP-1, Bay Carbon) using the modified Hummers' method. The graphite powder (2.0 g) was put into an 80 °C solution of concentrated H_2SO_4 (3.0 mL), $K_2S_2O_8$ (1.0 g), and P_2O_5 (1.0 g). The resultant dark blue mixture was thermally isolated and allowed to cool to room temperature

over a period of 6 h. The mixture was then carefully diluted with distilled water, filtered, and washed on the filter until the pH of the rinsewater became neutral. The product was dried in air at ambient temperature overnight. This preoxidized graphite was then subjected to oxidation by the Hummers' method. The preoxidized graphite powder (2.0 g) was put into cold concentrated H_2SO_4 (46 mL). $KMnO_4$ (6.0 g) was added gradually with

stirring and cooling, and the temperature of the mixture was not allowed to reach 20 °C. The mixture was then stirred at 35 °C for 2 h, and distilled water (92 mL) was added. After 15 min, the reaction was terminated by the addition of a large amount of distilled water (280 mL) and a 30% H_2O_2 solution (5.0 mL), after which the color of the mixture changed to bright yellow. The mixture was filtered and washed with a 1:10 HCl solution (500 mL) in order to remove metal ions. The graphite oxide product was suspended in distilled water to give a viscous, brown dispersion, which was subjected to dialysis to completely remove metal ions and acids. Exfoliation of the above graphite oxide to graphene oxide was carried out by dilution of the concentrated graphite oxide dispersion (3.5 mL) with deionized water (35 mL), followed by vigorous stirring at 15 000 rpm with a homogenizer for 15 min and ultrasonication for 10 min. The resulting homogeneous yellow-brown sol, of which the concentration is 0.5 mg/mL, was stable for at least a few months.

Preparation of Positively Charged G-O. Positively charged G-O was synthesized using N-ethyl-N′-(3-dimethylaminopropyl-)carbodiimidemethiodide (EDC, 98%, Alfa Aesar) and ethylenediamine (99%, Sigma-Aldrich).[29] First, concentrated graphite oxide solution (10 mL) was diluted and dispersed in deionized water by ultrasonication treatment for 30 min. Then, 50 mL of G-O suspension (0.5 mg/mL) was combined with EDC (600 mg) and ethylenediamine (4 mL) and stirred for 4 h, and afterward the mixture solution was dialyzed for 24 h to remove EDC and ethylenediamine. The MWCO of the dialysis tubing (Spectra/Por dialysis membrane) was 12−14 kD. Then a positively charged, dark brown G-O suspension was obtained.

Fabrication of G-O Thin Films Using a Layer-by-Layer Assembly. SiO_2 of 300 nm deposited on a Si substrate was cleaned by acetone with ultrasonication to remove any organic contamination and treated by oxygen plasma to introduce a hydrophilic surface. A positively charged G-O solution (0.5 mg/mL) at pH 3.7 was dropped on the 300 nm SiO_2 deposited on a Si substrate, which was loaded in a spin coater (ACE-200, Dong Ah Tech), maintained for 60 s as a waiting period, and spun at 3000 rpm for 60 s. As a rinsing step, DI water at the same pH was dropped on the substrate coated with positively charged G-O, maintained for 60 s, and spun at 3000 rpm for 60 s. Next, a negatively charged G-O solution (0.5 mg/mL) at pH 10 was spin-coated with the same procedures, followed by the rinsing step. Then, we obtained one bilayer of G-O sheets. These processes for one bilayer were repeated to make five, seven, or nine bilayers. While the thermal reduction method has some advantages, namely, its process time is shorter than vapor reduction and it is not necessary to use molecules harmful to humans and the environment, high temperature is required for sufficient reduction. In this study, the thermal reduction of G-O to make rG-O was generally done at temperatures of 200−1100 °C in the flow of Ar and H_2 gases for effective reduction and prevention of oxidative damage. We used a gas flow of a total of 100 sccm with a gas volume ratio of 90 sccm Ar and 10 sccm H_2. First of all, the tube furnace was fully evacuated by rotary pump over 15 min and the inner pressure of the tube needed to be below 1×10^{-3} Torr before increasing the furnace temperature to prevent oxidative damage from a quite small amount of residual oxygen in the tube. After it was fully evacuated to low pressure, Ar and H_2 gases were flowed down into the tube furnace under precise control of the gas volume ratio through a mass flow controller over 10 min to make an inert atmosphere, and then the furnace temperature was increased to 200−1100 at 20 °C/min of the heating rate for the thermal reduction. After the temperature reached 200−1100 °C, the G-O samples were maintained at that temperature for 1 h and then slowly cooled, maintaining the inert conditions with the flow of Ar and H_2 gases.

Transfer of the rG-O Thin Film to the Metal Surface. The fabricated rG-O thin film on 300 nm SiO_2 deposited on a Si substrate needed to be transferred to Cu or Fe foil to test their ability of oxidation resistance (Figure 1). First of all, the rG-O thin film was supported by poly(methyl methacrylate) (PMMA), which is commonly used as a supporting layer for the transfer of CVD-grown graphene or rG-O thin films because it is robust and easily removed by acetone after the transfer. In this study, an e-beam resist (AR-P 671.04, ALLRESIST) was used as a PMMA supporting layer and coated by spin-coating at 3000 rpm for 30 s. Then, the PMMA-supported rG-O thin film (PMMA/rG-O) on 300 nm SiO_2 deposited on a Si wafer was floated in 5 wt % hydrogen fluoride (HF) solution to detach PMMA/rG-O from the substrate by removing a SiO_2 layer. The detached PMMA/rG-O was washed out more than three times to eliminate the residual HF acid molecules in their interlayer and transferred onto Fe or Cu foils. The PMMA/rG-O-coated foils were put into acetone for 1 h to remove the PMMA layers.

Characterization. The average size and morphology of the G-O sheets were measured by SEM (Nanonova 230, FEI) and AFM (D3100 Nanoscope V, Veeco). The thickness of G-O and rG-O multilayers on a 300 nm thick SiO_2-on-Si wafer was characterized by ellipsometry (EC-400 and M-2000 V, J. A. Woollam Co. Inc.). Surface charges of the samples were measured by a ζ-potential analyzer (Malvern, Zetasizer Nano ZS) in a pH range of 2.5−10. Identification of elements and functional groups and degree of reduction of G-O sheets were done by XPS with a monochromatic Al Kα X-ray source (K-Alpha, Thermo Fisher). The G-O and rG-O multilayers and metal oxide formation were investigated by Raman spectroscopy (Alpha 300S, WITec) with a 532 nm excitation wavelength (exposure time of 10 s and laser power of 30 mW).

REFERENCES AND NOTES

1. Segarra, M.; Miralles, L.; Diaz, J.; Xuriguera, H.; Chimenos, J.; Espiell, F.; Pinol, S. Copper and CuNi Alloys Substrates for HTS Coated Conductor Applications Protected from Oxidation. *Mater. Sci. Forum* **2003**, *426*, 3511–3516.
2. Grundmeier, G.; Reinartz, C.; Rohwerder, M.; Stratmann, M. Corrosion Properties of Chemically Modified Metal Surfaces. *Electrochim. Acta* **1998**, *43*, 165–174.
3. Kinlen, P. J.; Menon, V.; Ding, Y. A Mechanistic Investigation of Polyaniline Corrosion Protection Using the Scanning Reference Electrode Technique. *J. Electrochem. Soc.* **1999**, *146*, 3690.
4. Mittal, V. K.; Bera, S.; Saravanan, T.; Sumathi, S.; Krishnan, R.; Rangarajan, S.; Velmurugan, S.; Narasimhan, S. V. Formation and Characterization of Bi-Layer Oxide Coating on Carbon-Steel for Improving Corrosion Resistance. *Thin Solid Films* **2009**, *517*, 1672–1676.
5. Stratmann, M.; Feser, R.; Leng, A. Corrosion Protection by Organic Films. *Electrochim. Acta* **1994**, *39*, 1207–1214.
6. Gray, J. E.; Luan, B. Protective Coatings on Magnesium and Its Alloys—a Critical Review. *J. Alloys Compd.* **2002**, *336*, 88–113.
7. Redondo, M.; Breslin, C. Polypyrrole Electrodeposited on Copper from an Aqueous Phosphate Solution: Corrosion Protection Properties. *Corros. Sci.* **2007**, *49*, 1765–1776.
8. Appa Rao, B. V.; Yakub Iqbal, M.; Sreedhar, B. Self-Assembled Monolayer of 2-(Octadecylthio)Benzothiazole for Corrosion Protection of Copper. *Corros. Sci.* **2009**, *51*, 1441–1452.
9. Bae, S.; Kim, H.; Lee, Y.; Xu, X.; Park, J.-S.; Zheng, Y.; Balakrishnan, J.; Lei, T.; Ri Kim, H.; Song, Y. I.; *et al*. Roll-to-Roll Production of 30-Inch Graphene Films for Transparent Electrodes. *Nat. Nanotechnol.* **2010**, *5*, 574–578.

10. Chen, S.; Brown, L.; Levendorf, M.; Cai, W.; Ju, S.-Y.; Edgeworth, J.; Li, X.; Magnuson, C. W.; Velamakanni, A.; Piner, R. D.; *et al*. Oxidation Resistance of Graphene-Coated Cu and Cu/Ni Alloy. *ACS Nano* **2011**, *5*, 1321–1327.

11. Prasai, D.; Tuberquia, J. C.; Harl, R. R.; Jennings, G. K.; Bolotin, K. I. Graphene: Corrosion-Inhibiting Coating. *ACS Nano* **2012**, *6*, 1102–1108.

12. Kondo, D.; Sato, S.; Yagi, K.; Harada, N.; Sato, M.; Nihei, M.; Yokoyama, N. Low-Temperature Synthesis of Graphene and Fabrication of Top-Gated Field Effect Transistors without Using Transfer Processes. *Appl. Phys. Express* **2010**, *3*, 5102.

13. An, H.; Lee, W.-J.; Jung, J. Graphene Synthesis on Fe Foil Using Thermal CVD. *Curr. Appl. Phys.* **2011**, *11*, S81–S85.

14. Liu, N.; Fu, L.; Dai, B.; Yan, K.; Liu, X.; Zhao, R.; Zhang, Y.; Liu, Z. Universal Segregation Growth Approach to Wafer-Size Graphene from Non-Noble Metals. *Nano Lett.* **2010**, *11*, 297–303.

15. Eda, G.; Fanchini, G.; Chhowalla, M. Large-Area Ultrathin Films of Reduced Graphene Oxide as a Transparent and Flexible Electronic Material. *Nat. Nanotechnol.* **2008**, *3*, 270–274.

16. Dreyer, D. R.; Park, S.; Bielawski, C. W.; Ruoff, R. S. The Chemistry of Graphene Oxide. *Chem. Soc. Rev.* **2009**, *39*, 228–240.

17. Li, X.; Wang, H.; Robinson, J. T.; Sanchez, H.; Diankov, G.; Dai, H. Simultaneous Nitrogen Doping and Reduction of Graphene Oxide. *J. Am. Chem. Soc.* **2009**, *131*, 15939–15944.

18. Becerril, H. c. A.; Stoltenberg, R. M.; Tang, M. L.; Roberts, M. E.; Liu, Z.; Chen, Y.; Kim, D. H.; Lee, B.-L.; Lee, S.; Bao, Z. Fabrication and Evaluation of Solution-Processed Reduced Graphene Oxide Electrodes for P- and N-Channel Bottom-Contact Organic Thin-Film Transistors. *ACS Nano* **2010**, *4*, 6343–6352.

19. Stankovich, S.; Dikin, D. A.; Piner, R. D.; Kohlhaas, K. A.; Kleinhammes, A.; Jia, Y.; Wu, Y.; Nguyen, S. T.; Ruoff, R. S. Synthesis of Graphene-Based Nanosheets *via* Chemical Reduction of Exfoliated Graphite Oxide. *Carbon* **2007**, *45*, 1558–1565.

20. Wang, X.; Zhi, L.; Mullen, K. Transparent, Conductive Graphene Electrodes for Dye-Sensitized Solar Cells. *Nano Lett.* **2007**, *8*, 323–327.

21. Becerril, H. A.; Mao, J.; Liu, Z.; Stoltenberg, R. M.; Bao, Z.; Chen, Y. Evaluation of Solution-Processed Reduced Graphene Oxide Films as Transparent Conductors. *ACS Nano* **2008**, *2*, 463–470.

22. Cote, L. J.; Kim, F.; Huang, J. Langmuir−Blodgett Assembly of Graphite Oxide Single Layers. *J. Am. Chem. Soc.* **2008**, *131*, 1043–1049.

23. Zhu, Y.; Cai, W.; Piner, R. D.; Velamakanni, A.; Ruoff, R. S. Transparent Self-Assembled Films of Reduced Graphene Oxide Platelets. *Appl. Phys. Lett.* **2009**, *95*, 103104.

24. De, S.; King, P. J.; Lotya, M.; O'Neill, A.; Doherty, E. M.; Hernandez, Y.; Duesberg, G. S.; Coleman, J. N. Flexible, Transparent, Conducting Films of Randomly Stacked Graphene from Surfactant-Stabilized, Oxide-Free Graphene Dispersions. *Small* **2010**, *6*, 458–464.

25. Mohanty, N.; Berry, V. Graphene-Based Single-Bacterium Resolution Biodevice and DNA Transistor: Interfacing Graphene Derivatives with Nanoscale and Microscale Biocomponents. *Nano Lett.* **2008**, *8*, 4469–4476.

26. Ohno, Y.; Maehashi, K.; Yamashiro, Y.; Matsumoto, K. Electrolyte-Gated Graphene Field-Effect Transistors for Detecting pH and Protein Adsorption. *Nano Lett.* **2009**, *9*, 3318–3322.

27. Stoller, M. D.; Park, S.; Zhu, Y.; An, J.; Ruoff, R. S. Graphene-Based Ultracapacitors. *Nano Lett.* **2008**, *8*, 3498–3502.

28. Decher, G. Fuzzy Nanoassemblies: Toward Layered Polymeric Multicomposites. *Science* **1997**, *277*, 1232–1237.

29. Lee, D. W.; Hong, T.-K.; Kang, D.; Lee, J.; Heo, M.; Kim, J. Y.; Kim, B.-S.; Shin, H. S. Highly Controllable Transparent and Conducting Thin Films Using Layer-by-Layer Assembly of Oppositely Charged Reduced Graphene Oxides. *J. Mater. Chem.* **2011**, *21*, 3438–3442.

30. Hummers, W. S.; Offeman, R. E. Preparation of Graphitic Oxide. *J. Am. Chem. Soc.* **1958**, *80*, 1339–1339.

31. Mattevi, C.; Eda, G.; Agnoli, S.; Miller, S.; Mkhoyan, K. A.; Celik, O.; Mastrogiovanni, D.; Granozzi, G.; Garfunkel, E.; Chhowalla, M. Evolution of Electrical, Chemical, and Structural Properties of Transparent and Conducting Chemically Derived Graphene Thin Films. *Adv. Funct. Mater.* **2009**, *19*, 2577–2583.

32. Kudin, K. N.; Ozbas, B.; Schniepp, H. C.; Prud'Homme, R. K.; Aksay, I. A.; Car, R. Raman Spectra of Graphite Oxide and Functionalized Graphene Sheets. *Nano Lett.* **2008**, *8*, 36–41.

33. Thibeau, R. J.; Brown, C. W.; Heidersbach, R. H. Raman Spectra of Possible Corrosion Products of Iron. *Appl. Spectrosc.* **1978**, *32*, 532–535.

34. Oh, S. J.; Cook, D.; Townsend, H. Characterization of Iron Oxides Commonly Formed as Corrosion Products on Steel. *Hyperfine Interact.* **1998**, *112*, 59–66.

35. Nair, R. R.; Wu, H. A.; Jayaram, P. N.; Grigorieva, I. V.; Geim, A. K. Unimpeded Permeation of Water through Helium-Leak-Tight Graphene-Based Membranes. *Science* **2012**, *335*, 442–444.

36. Wang, S.; Zhang, Y.; Abidi, N.; Cabrales, L. Wettability and Surface Free Energy of Graphene Films. *Langmuir* **2009**, *25*, 11078–11081.

37. Shin, Y. J.; Wang, Y.; Huang, H.; Kalon, G.; Wee, A. T. S.; Shen, Z.; Bhatia, C. S.; Yang, H. Surface-Energy Engineering of Graphene. *Langmuir* **2010**, *26*, 3798–3802.

38. Niaura, G. Surface-Enhanced Raman Spectroscopic Observation of Two Kinds of Adsorbed OH-Ions at Copper Electrode. *Electrochim. Acta* **2000**, *45*, 3507–3519.

39. Chou, M.; Liu, S.; Huang, C.; Wu, S.; Cheng, C. L. Confocal Raman Spectroscopic Mapping Studies on a Single Cuo Nanowire. *Appl. Surf. Sci.* **2008**, *254*, 7539–7543.